DOI: 10.1021/ic902483m

Inorganic Chemistry
Article

Four Novel Frameworks Built by Imidazole-Based Dicarboxylate Ligands: Hydro(Solvo)thermal Synthesis, Crystal Structures, and Properties

Fuwei Zhang, Zifeng Li, Tiezhu Ge, Hongchang Yao, Gang Li,* Huijie Lu, and Yanyan Zhu

Department of Chemistry, Zhengzhou University, Henan 450052, People's Republic of China

Received December 18, 2009

Four novel complexes, $\{[Ni_4(HEIDC)_4(H_2O)_8]\cdot 2H_2O\}$ (**1**), $\{[Mn(HEIDC)(4,4'\text{-bipy})_{0.5}(H_2O)]\cdot H_2O\}_n$ (**2**), $[Mn_6(EIDC)_4(py)(H_2O)_4]_n$ (**3**), and $\{[Cd_2(EIDC)(H_2EIDC)(4,4'\text{-bipy})_{1.5}]\cdot H_2O\}_n$ (**4**) (H_3EIDC = 2-ethyl-1*H*-imidazole-4,5-dicarboxylic acid, 4,4′-bipy = 4,4′-bipyridine, and py = pyridine) have been hydro(solvo)thermally synthesized by fine control over synthetic conditions, such as solvent and pH value, and structurally characterized. It is shown through single-crystal X-ray diffractions that the ligands H_3EIDC can be either singly, doubly, or triply deprotonated and can coordinate to Ni(II), Mn(II) or Cd(II) ions in μ_2 or μ_3 modes. Compound **1** is a zero-dimensional (0D) symmetrical tetranuclear molecular square. Compound **2** exhibits a two-dimensional (2D) sheet, in which alternate left- and right-handed helical chains are bridged by 4,4′-bipy linkages. Compound **3** assumes a 2D honeycomb-like sheet built up from μ_3-$EIDC^{3-}$ and Mn(II) atoms. Compound **4** possesses a novel three-dimensional (3D) structure constructed from 2D layer motifs joined by μ_2-$HEIDC^{2-}$ and 4,4′-bipy bridges. The thermal properties of complexes **1**−**4** have been determined as well. Also, it is discovered that there exists antiferromagnetic coupling between the Ni(II) or Mn(II) ions in **1** or **2** (**3**); the best fittings to the experimental magnetic susceptibilities gave $J = -10.83$ cm^{-1} and $g = 2.19$ for **1**, and $J = -0.025$ cm^{-1}, $zJ' = -0.02$ cm^{-1} and $g = 2.0$ for **2**.

Introduction

In recent years, increasing attention has been paid to the design and synthesis of metal−organic frameworks (MOFs), not only owing to their intriguing variety of architectures but also because of their potential applications as microporous, magnetic, nonlinear optical, and fluorescent materials.[1] Generally, the preparation of such materials can be influenced by many factors, such as the nature of organic ligands, the coordination preference of central metal ion, the crystallization conditions, the metal/ligand ratio, and the reaction solvent system, etc.[2] It is well-known that the multifunctional organic ligands play an important role in directing the extended structure of the resulting complexes, which can effectively construct MOFs with unique structures and properties. Thus, considerable efforts have been devoted to choose or design various multifunctional bridging ligands.[3]

Recently, heterocyclic dicarboxylate ligands have attracted much attention in preparation of interesting polymeric frameworks due to their outstanding features of various coordination fashions under hydrothermal condition.[4] In this context, imidazole-4,5-dicarboxylic acid (H_3IDC) becomes an excellent candidate for assembling novel MOFs by incorporating appropriate metal ions in different ways. The reported MOFs based on H_3IDC possess beautiful and interesting topological structures, for

*Corresponding author. Fax: +86-371-67766109. E-mail: gangli@zzu.edu.cn.

(1) (a) Morsali, A.; Masoomi, M. Y. *Coord. Chem. Rev*. **2009**, *253*, 1882. (b) Rao, C. N. R.; Natarajan, S.; Vaidhyanathan, R. *Angew. Chem., Int. Ed. Engl*. **2004**, *43*, 1466. (c) Zhang, J.; Li, Z.-J.; Kang, Y.; Cheng, J.-K.; Yao, Y.-G. *Inorg. Chem*. **2004**, *43*, 8085. (d) Tong, M.-L.; Chen, X.-M.; Ye, B.-H.; Ji, L.-N. *Angew. Chem., Int. Ed. Engl*. **1999**, *38*, 2237. (e) Lin, J.-D.; Cheng, J.-W.; Du, S.-W. *Cryst. Growth Des*. **2008**, *8*, 3345. (f) Alkordi, M. H.; Liu, Y.-L.; Larsen, R. W.; Eubank, J. F.; Eddaoudi, M. *J. Am. Chem. Soc*. **2008**, *130*, 12639. (g) Miyasaka, H.; Ieda, H.; Matsumoto, N.; Sugiura, K.; Yamashita, M. *Inorg. Chem*. **2003**, *42*, 3509. (h) Wu, C.-D.; Ma, L.; Lin, W. *Inorg. Chem*. **2008**, *47*, 11446. (i) Kirillov, A. M.; Karabach, Y. Y.; Haukka, M.; Guedes da Silva, M. F. C.; Sanchiz, J.; Kopylovich, M. N.; Pombeiro, A. J. L. *Inorg. Chem*. **2008**, *47*, 162. (j) Zhang, J.-P.; Lin, Y.-Y.; Huang, X.-C.; Cheng, X.-M. *J. Am. Chem. Soc*. **2009**, *127*, 5495. (k) Hou, H.-W.; Meng, X.-R.; Song, Y.-L.; Fan, Y.-T.; Lu, H.-J.; Du, C.-X.; Shao, W.-H. *Inorg. Chem*. **2002**, *41*, 4068. (l) García-Couceiro, U.; Castillo, O.; Luque, A.; García-Terán, J. P.; Beobide, G.; Román, P. *Cryst. Growth Des*. **2006**, *6*, 1839.

(2) (a) Song, Y. J.; Kwak, H.; Lee, Y. M.; Kim, S. H.; Lee, S. H.; Park, B. K.; Jun, J. Y.; Yu, S. M.; Kim, C.l; Kim, S.-J.; Kim, Y. *Polyhedron* **2009**, *28*, 1241. (b) Tong, M.-L.; Kitagawa, S.; Chang, H.-C.; Ohba, M. *Chem. Commun*. **2004**, 41841. (c) Du, M.; Wang, X.-G.; Zhang, Z.-H.; Tang, L.-F.; Zhao, X.-J. *CrystEngComm* **2006**, *8*, 788. (d) Moulton, B.; Zaworotko, M. J. *Chem. Rev*. **2001**, *101*, 1629. (e) Varughese, S.; Pedireddi, V. R. *Chem. Commun*. **2005**, 1824. (f) Plater, M. J.; Foreman, M. R. S. J.; Gelbrich, T.; Coles, S. J.; Hursthouse, M. B. *J. Chem. Soc., Dalton Trans*. **2000**, 3065. (g) Rosi, N. L.; Eddaoudi, M.; Kim, J.; O'Keeffe, M.; Yaghi, O. M. *Angew. Chem., Int Ed. Engl*. **2002**, *41*, 284. (h) Wu, A.-Q.; Li, Y.; Zheng, F.-K.; Guo, G.-C.; Huang, J.-S. *Cryst. Growth Des*. **2006**, *6*, 444. (i) Lei, X. J.; Shang, M. Y.; Patil, A.; Wolf, E. E.; Fehlner, T. P. *Inorg. Chem*. **1996**, *35*, 3217. (j) Wen, Y.-H.; Cheng, J.-K; Feng, Y.-L.; Zhang, J.; Li, Z.-J.; Yao, Y.-G. *Inorg. Chim. Acta* **2005**, *358*, 3347. (k) Ren, P.; Xu, N.; Chen, C.; Song, H.-B.; Shi, W.; Cheng, P. *Inorg. Chem. Commun*. **2008**, *11*, 730. (l) Cao, R.; Sun, D.-F.; Liang, Y.-C.; Hong, M.-C.; Tatsumi, K.; Shi, Q. *Inorg. Chem*. **2002**, *41*, 2087. (m) Hong, C.-S.; Son, S.-K.; Lee, Y. S.; Jun, M.-J.; Do, Y. *Inorg. Chem*. **1999**, *38*, 5602. (n) Wang, Y.-T.; Tong, M.-L.; Fan, H.-H.; Wang, H.-Z.; Chen, X.-M. *Dalton Trans*. **2005**, 424. (o) Chen, C. Y.; Cheng, P. Y.; Wu, H. H.; Lee, H. M. *Inorg. Chem*. **2007**, *46*, 5691. (p) Phuengphai, P.; Youngme, S.; Kongsaeree, P.; Pakawatchai, C.; Chaichit, N.; Teat, S. J.; Gamez, P.; Reedijk, J. *CrystEngComm* **2009**, *11*, 1723.

Published on Web 03/15/2010

instance one-dimensional (1D) chains, two-dimensional (2D) sheets, three-dimensional (3D) porous structures, and interpenetrating networks. It has been found that the ligand H_3IDC not only can be partially or fully deprotonated to H_2IDC^-, $HIDC^{2-}$, and IDC^{3-} but also exhibits very flexible coordination modes.[5] These interesting findings have prompted us to seek more similar ligands to synthesize more desired complexes. Thus, we chose one analogue ligand, 2-ethyl-1*H*-imidazole-4,5-dicarboxylic acid (H_3EIDC) with an ethyl substituent in the two-position of the imidazole group, because it may introduce additional structural constrain in controlling the assembly of metal-organic networks. By doing so, we hope to reveal some structural factors of the ligand H_3EIDC for dominating the self-assembly, and this will provide more useful information of the ethyl substituent effect in such a ligand.

In contrast to the well-studied ligand H_3IDC,[5] MOFs comprised of H_3EIDC are still rare. Indeed, to the best of our knowledge, only one single example of 3D Cd(II) coordination polymer was reported by Shuang and co-workers.[6] Herein, we report the hydro(solvo)thermal syntheses, structural determinations of four novel complexes, tetranuclear square $[Ni_4(HEIDC)_4(H_2O)_8]\cdot 2H_2O$ (**1**), 2D coordination polymers $\{[Mn(HEIDC)(4,4'\text{-bipy})_{0.5}(H_2O)]\cdot H_2O\}_n$ (**2**), $[Mn_6(EIDC)_4(py)_4(H_2O)_4]_n$ (**3**), and 3D coordination polymer $\{[Cd_2(EIDC)(H_2EIDC)(4,4'\text{-bipy})_{1.5}]\cdot H_2O\}_n$ (**4**) (4,4′-bipy = 4,4′-bipyridine, py = pyridine). Single crystal X-ray diffractions reveal that one to three hydrogen atoms can be removed from the ligand H_3EIDC forming H_2EIDC^-, $HEIDC^{2-}$, or $EIDC^{3-}$ anions, and the deprotonated $H_{3-n}EIDC^{n-}$ ($n = 1-3$) could coordinate to metal ions in μ_2 or μ_3 modes (Scheme 1). Their thermal and magnetic properties have been investigated also.

Experimental Section

General Details. All chemicals were of reagent grade quality obtained from commercial sources and used without further purification. The organic ligand H_3EIDC was prepared according to literature procedure.[7]

C, H, and N microanalyses were carried out on a FLASH EA 1112 analyzer. IR data were recorded on a BRUKER TENSOR 27 spectrophotometer with KBr pellets in the 400−4000 cm^{-1} region. TG-DSC measurements were performed by heating the sample from 20 to 800 °C at a rate of 10 °C·min^{-1} in air on a Netzsch STA 409PC differential thermal analyzer. Variable-temperature magnetic susceptibility data were obtained on a SQUID susceptometer (Quantum Design, MPMS-5) in the temperature range of 2.0−300 K with an applied field of 1000 G. All magnetic data have been corrected for diamagnetism by using Pascal′s constants.[8]

Preparation of Crystalline $[Ni_4(HEIDC)_4(H_2O)_8]\cdot 2H_2O$ (1). A mixture of H_3EIDC (36.8 mg, 0.2 mmol), $Ni(NO_3)_2\cdot 6H_2O$ (5.8 mg, 0.2 mmol), and EtOH/H_2O (6:1, 7 mL) was sealed in a 25 mL Teflon-lined bomb and heated at 150 °C for 96 h. The reaction mixture was then allowed to cool to room temperature at a rate of 10 °C/h. Block−shape crystals of **1** were collected, washed with methanol, and dried in air. Yield: 86%. Anal. calcd for $C_{28}H_{36}N_8O_{26}Ni_4$: C, 29.62; H, 3.17; N, 9.87%. Found: C, 30.02; H, 3.01; N, 9.48%. IR (cm^{-1}, KBr): 3479 s, 2985 w, 1571 s, 1273 m, 1130 m, 867 w, 784 m, 751 w, 493 w.

Preparation of Crystalline $\{[Mn(HEIDC)(4,4'\text{-bipy})_{0.5}(H_2O)]\cdot H_2O\}_n$ (2). A mixture of H_3EIDC (24.1 mg, 0.13 mmol), $MnSO_4\cdot H_2O$ (21.9 mg, 0.13 mmol), 4,4′-bipy (20.2 mg, 0.13 mmol), Et_3N (0.056 mL, 0.4 mmol), and deionized water (7 mL) was sealed in a 25 mL Teflon-lined bomb, which was heated to 150 °C for 96 h. After the mixture was cooled to room temperature at a rate of 10 °C/h, yellow crystals of **2** were obtained, washed with distilled water, and dried in air. Yield: 64%. Anal. calcd for $C_{12}H_{14}MnN_3O_6$: C, 41.27; H, 3.47; N, 12.04%. Found: C, 40.92; H, 4.03; N, 11.87%. IR (cm^{-1}, KBr): 3451 m, 3205 s, 2903 w, 1607 s, 1570 s, 1525 m, 1465 m, 1391 m, 1244 m, 1070 s, 813 m, 634 m.

Preparation of Crystalline $[Mn_6(EIDC)_4(py)_4(H_2O)_4]_n$ (3). A mixture of H_3EIDC (36.8 mg, 0.2 mmol), $Mn(OAc)_2$ (34.6 mg, 0.2 mmol), py (pyridine) (0.2 mL), and deionized water (7 mL)

(3) (a) Ghosh, S. K.; Bharadwaj, P. K. *Inorg. Chem.* **2004**, *43*, 2293. (b) Guo, H. D.; Guo, X. M.; Wang, X.; Guo, Z. Y.; Su, S. Q.; Zhang, H. J. *CrystEngComm* **2009**, *11*, 1509. (c) Chen, Z.-L.; Jiang, C.-F.; Yan, W.-H.; Liang, F.-P.; Batten, S. R. *Inorg. Chem.* **2009**, *48*, 4674. (d) Woodward, J. D.; Backov, R. V.; Abboud, K. A.; Talham, D. R. *Polyhedron* **2006**, *25*, 2605. (e) Mu, B.; Li, F.; Walton, K. S. *Chem. Commun.* **2009**, 2493. (f) Biradha, K.; Fujita, M. *J. Chem. Soc., Dalton Trans.* **2000**, 3805. (g) Wu, B.; Ren, Z.-G.; Li, H.-X.; Dai, M.; Li, D.-X; Zhang, Y.; Lang, J.-P. *Inorg. Chem. Commun.* **2009**, *12*, 1168. (h) Anokhina, E. V.; Jacobson, A. J. *J. Am. Chem. Soc.* **2004**, *126*, 3044. (i) Liu, G. F.; Ren, Z. J.; Chen, Y.; Liu, D.; Li, H. X.; Zhang, Y.; Lang, J. P. *Inorg. Chem. Commun.* **2008**, *11*, 221. (j) Hou, H. W.; Fan, Y. T.; Zhang, L. P.; Du, C. X.; Zhu, Y. *Inorg. Chem. Commun.* **2001**, *4*, 168. (k) Hou, H. W.; Song, Y. L.; Fan, Y. T.; Zhang, L. P.; Du, C. X.; Zhu, Y. *Inorg. Chim. Acta* **2001**, *316*, 140. (l) Wu, S. T.; Long, L. S.; Huang, R. B.; Zheng, L. S. *Cryst. Growth Des.* **2007**, *7*, 1746. (m) Tao, J.; Zhang, Y.; Tong, M.-L.; Chen, X.-M.; Yuen, T.; Lin, C.-L.; Huang, X.-Y.; Li, J. *Chem. Commun.* **2002**, 1342.

(4) (a) Tian, G.; Zhu, G. S.; Yang, X. Y.; Fang, Q. R.; Xue, M.; Sun, J. Y.; Wei, Y.; Qiu, S. L. *Chem. Commun.* **2005**, 1396. (b) Zhao, B.; Chen, X.-Y.; Cheng, P.; Liao, D.-Z.; Yan, S.-P; Jiang, Z.-H. *J. Am. Chem. Soc.* **2004**, *126*, 15394. (c) Lang, X.-Q.; Chen, C.; Zhou, X.-H.; Xiao, H.-P.; Li, Y.-Z.; Zuo, J.-L.; You, X.-Z. *Polyhedron* **2009**, *28*, 947. (d) Lin, X.; Blake, A. J.; Wilson, C.; Sun, X.-Z.; Champness, N. R.; George, M. W.; Hubberstey, P.; Mokaya, R.; Schroeder, M. *J. Am. Chem. Soc.* **2006**, *128*, 10745. (e) Liu, Y.-L.; Kravtsov, V. C.; Beauchamp, D. A.; Eubank, J. F.; Eddaoudi *J. Am. Chem. Soc.* **2005**, *127*, 7266. (f) Zhao, X. Q.; Zhao, B.; Shi, W.; Cheng, P.; Liao, D. Z.; Yan, S. P. *Dalton Trans.* **2009**, 2281. (g) Eubank, J. F.; Walsh, R. D.; Poddar, P.; Srikanth, H.; Larsen, R. W.; Eddaoudi, M. *Cryst. Growth Des.* **2006**, *6*, 1453. (h) Yue, Y.-F.; Liang, J.; Gao, E.-Q.; Yan, Z.-G.; Yan, C.-H. *Inorg. Chem.* **2008**, *47*, 6115. (i) Bai, Z.-S.; Qi, Z.-P.; Lu, Y.; Yuan, Q.; Sun, W.-Y. *Cryst. Growth Des.* **2008**, *8*, 1924. (j) Shi, W.; Chen, X. Y.; Xu, X. N.; Song, S. B.; Zhao, B.; Cheng, P.; Liao, D. Z.; Yan, S. P. *Eur. J. Inorg. Chem.* **2006**, 4931. (k) Zhao, X.-Q.; Zhao, B.; Ma, Y.; Shi, W.; Cheng, P.; Jiang, Z.-H.; Liao, D.-Z.; Yan, S.-P. *Inorg. Chem.* **2007**, *46*, 5832. (l) Zhao, B.; Cheng, P.; Chen, X. Y.; Cheng, C.; Shi, S.; Wang, D. Z.; Yan, S. P.; Jiang, Z. H. *J. Am. Chem. Soc.* **2004**, *126*, 3012. (m) MacGillivray, L. R.; Groeneman, R. H.; Atwood, J. L. *J. Am. Chem. Soc.* **1998**, *120*, 2676. (n) Nie, X. L.; Wen, H. L.; Wu, Z. S.; Liu, D. B.; Liu, C. B. *Acta Crystallogr., Sect. E: Struct. Rep. Online* **2007**, *63*, m753.

(5) (a) Sun, Y.-Q.; Zhang, J.; Chen, Y.-M.; Yang, G.-Y. *Angew. Chem., Int. Ed. Engl.* **2005**, *44*, 5814. (b) Maji, T. K.; Mostafa, G.; Chang, H.-C.; Kitagawa, S. *Chem. Commun.* **2005**, *9*, 2436. (c) Liu, Y.-L.; Kravtsov, V.; Walsh, R. D.; Poddar, P.; Srikanth, H.; Eddaoudi, M. *Chem. Commun.* **2004**, *24*, 2806. (d) Lu, W.-G.; Su, C.-Y.; Lu, T.-B.; Jiang, L.; Chen, J.-M. *J. Am. Chem. Soc.* **2006**, *128*, 34. (e) Liu, Y.-L; Kravtsov, V. C.; Larsen, R.; Eddaoudi, M. *Chem. Commun.* **2006**, *14*, 1488. (f) Zou, R.-Q.; Jiang, L.; Senoh, H.; Takeichi, N.; Xu, Q. *Chem. Commun.* **2005**, *28*, 3526. (g) Lu, J. Y.; Ge, Z. H. *Inorg. Chim. Acta* **2005**, *358*, 828. (h) Zhang, X. F.; Huang, D. G.; Chen, F.; Chen, D. G.; Liu, Q. T. *Inorg. Chem. Commun.* **2004**, *7*, 662. (i) Zhao, B.; Zhao, X. Q.; Shi, W.; Cheng, P. *J. Mol. Struct.* **2007**, *830*, 143. (j) Rajendiran, T. M.; Kirk, M. L.; Setyawati, I. A.; Caudle, M. T.; Kampf, J. W.; Pecoraro, V. L. *Chem. Commun.* **2003**, *7*, 824. (k) Plieger, P. G.; Ehler, D.-S.; Duran, B.-L.; Taylor, T. P.; John, K. D.; Keizer, T. S.; McCleskey, T. M.; Burrell, A. K.; Kampf, J. W.; Haase, T.; Rasmussen, P. G.; Karr, J. *Inorg. Chem.* **2005**, *44*, 5761. (l) Li, C.-J.; Hu, S.; Li, W.; Lam, C. K.; Zheng, Y.-Z.; Tong, M.-L. *Eur. J. Inorg. Chem.* **2006**, 1931. (m) Gu, J.-Z.; Lu, W.-G.; Jiang, L.; Zhou, H.-C.; Lu, T.-B. *Inorg. Chem.* **2007**, *46*, 5835. (n) Fang, R.-Q.; Zhang, X.-M. *Inorg. Chem.* **2006**, *45*, 4801. (o) Fang, R. Q.; Zhang, X. H.; Zhang, X. M. *Cryst. Growth Des.* **2006**, *6*, 2637. (p) Zhang, M. B.; Chen, Y. M.; Zheng, S. T.; Yang, G. Y. *Eur. J. Inorg. Chem.* **2006**, 1423. (q) Xu, Q.; Zou, R.-Q.; Zhong, R.-Q.; Kachi-Terajima, C.; Takamizawa, S. *Cryst. Growth Des.* **2008**, *8*, 2458.

(6) Wang, S.; Zhang, L. R.; Li, G. H.; Huo, Q. S.; Liu, Y. L. *CrystEngComm* **2008**, *10*, 1662.

(7) (a) Sun, T.; Ma, J. P.; Huang, R. Q.; Dong, Y. B. *Acta Crystallogr., Sect. E: Struct. Rep. Online* **2006**, *62*, o6751. (b) Alcalde, E.; Dinares, I.; Perez-Garcia, L.; Roca, T. *Synthesis* **1992**, 395.

(8) Carlin, R. L. *Magnetochemistry*, Springer: New York, 1986.

Scheme 1. Coordination Modes of $H_{3-n}EIDC^{n-}$ Anions (n = 1−3)

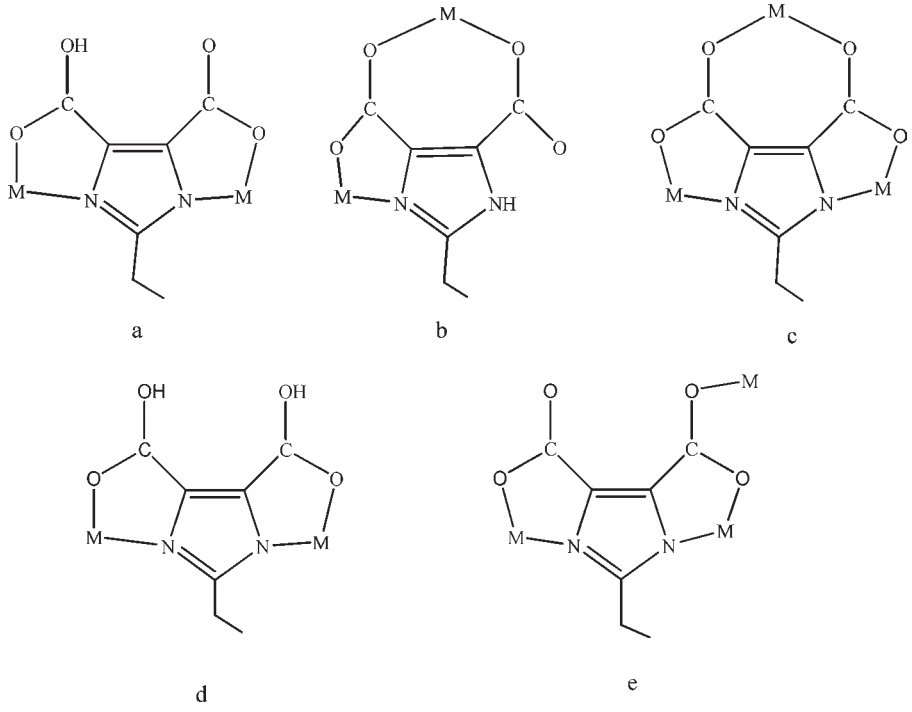

was sealed in a 25 mL Teflon-lined bomb and heated at 160 °C for 96 h, and then cooled to room temperature at a rate of 10 °C/h. Colorless flake-shaped crystals of **3** were collected, washed with distilled water, and dried in air. Yield: 53% (based on H_3EIDC). Anal. calcd for $C_{48}H_{48}N_{12}O_{20}Mn_6$: C, 39.96; H, 3.32; N, 11.65%. Found: C, 39.78; H, 3.52; N, 11.42%. IR (cm^{-1}, KBr): 3440 s, 2847 w, 1570 s, 1446 w, 1374 w, 1245 w, 1221 w, 837 s, 699 s.

Preparation of Crystalline $\{[Cd_2(EIDC)(H_2EIDC)(4,4'\text{-bipy})_{1.5}]\cdot H_2O\}_n$ (4). A mixture of H_3EIDC (36.8 mg, 0.2 mmol), $Cd(NO_3)_2\cdot 4H_2O$ (61.6 mg, 0.2 mmol), py (0.2 mL), 4,4′-bipy (31.2 mg, 0.2 mmol), and deionized water (7 mL) was sealed in a 25 mL Teflon-lined bomb and heated at 160 °C for 96 h, and then cooled to room temperature at a rate of 10 °C/h. Good-quality colorless crystals for **4** were filtered off, washed with water, and dried in air. Crystals of **4** are stable in the air. Yield: 56%. Anal. calcd. for $C_{29}H_{24}N_7O_9Cd_2$: C, 41.49; H, 2.85; N, 11.68%. Found: C, 41.15; H, 2.53; N, 11.48%. IR (cm^{-1}, KBr): 3472 s, 1604 w, 1538 m, 1393 s, 1262 s, 1221 s, 1121 m, 1066 s, 1009 w, 859 w, 821 w.

X-ray Crystallography. Crystal data and experimental details for compounds **1**−**4** are contained in Table 1. Measurements of compounds **1**−**3** were made on a Rigaku Saturn 724+ CCD diffractometer with a graphite-monochromated Mo Kα radiation (λ = 0.71073 Å). Polymer **4** was measured on a Rigaku RAXIS-IV imaging plate area detector with graphite-monochromated Mo Kα radiation (λ = 0.71073 Å). Single crystals of **1**−**4** were selected and mounted on a glass fiber. All data were collected at room temperature using the ω-2θ scan technique and corrected for Lorenz-polarization effects. A correction for secondary extinction was applied.

The four structures were solved by direct methods and expanded using the Fourier technique. The non-hydrogen atoms were refined with anisotropic thermal parameters. Hydrogen atoms were included but not refined. The final cycle of full-matrix least-squares refinement was based on 958 observed reflections and 89 variable parameters for **1**, 3150 observed reflections and 218 variable parameters for **2**, 10 286 observed reflections and 231 variable parameters for **3**, and 6613 observed reflections and 422 variable parameters for **4**. All calculations were performed using the SHELX-97 crystallographic software package.[9a] Selected bond lengths and angles are listed in Table 2.

Quantum-Chemical Calculation. The optimized geometries, the Mulliken atomic charge distributions, and the energies of the frontier molecular orbitals of the free ligands were given by the GAUSSIAN 03 suite of programs.[9b] And all calculations were carried out at the B3LYP/6-311++G(d, p) level of theory.

Results and Discussion

Crystal Structures of Crystalline Tetranuclear Square $[Ni_4(HEIDC)_4(H_2O)_8]\cdot 2H_2O$ (1). The molecular structure of **1** can be viewed as being made up of a $[Ni_4(HEIDC)_4(H_2O)_8]$ unit and two noncoordinated water molecules, which exhibits an interesting molecular square conformation.

As is shown in Figure 1a, each Ni(II) atom is six-coordinated and adopts a slightly distorted octahedral geometry. One of the equatorial planes is defined by oxygen atoms (O3 and O3A) from two coordinated water molecules and two nitrogen atoms (N1 and N1A) of two $HEIDC^{2-}$ ligands (the mean deviation from the plane

(9) (a) Sheldrick, G. M. *SHELX-97, Program for the Solution and Refinement of Crystal Structures*; University of Göttingen: Göttingen, Germany, 1997. (b) Frisch, M. J.; Trucks, G. W.; Schlegel, H. B.; Scuseria, G. E.; Robb, M. A.; Cheeseman, J. R.; Montgomery, J. A.; Vreven, T. J.; Kudin, K. N.; Burant, J. C.; Millam, J. M.; Iyengar, S. S.; Tomasi, J.; Barone, V.; Mennucci, B.; Cossi, M.; Scalmani, G.; Rega, N.; Petersson, G. A.; Nakatsuji, H.; Hada, M.; Ehara, M.; Toyota, K.; Fukuda,R.; Hasegawa, J.; Ishida, M.; Nakajima, T.; Honda, Y.; Kitao, O.; Nakai, H.; Klene, M.; Li, X.; Knox, J. E.; Hratchian, H. P.; Cross, J. B.; Bakken, V.; Adamo, C.; Jaramillo, J.; Gomperts, R.; Stratmann, R. E.; Yazyev, O.; Austin, A. J.; Cammi, R.; Pomelli, C.; Ochterski, J. W.; Ayala, P. Y.; Morokuma, K.; Voth, G. A.; Salvador, P.; Dannenberg, J. J.; Zakrzewski, V. G.; Dapprich, S.; Daniels, A. D.; Strain, M. C.; Farkas, O.; Malick, D. K.; Rabuck, A. D.; Raghavachari, K.; Foresman, J. B.; Ortiz, J. V.; Cui, Q.; Clifford, A. G.; Baboul, S.; Cioslowski, J.; Stefanov, B. B.; Liu, G.; Liashenko, A.; Piskorz, P.; Komaromi, I.; Martin, R. L.; Fox, D. J.; Keith, T.; Al-Laham, M. A.; Peng,C. Y.; Nanayakkara, A.; Challacombe, M.; Gill, P. M. W.; Johnson, B.; Chen, W.; Wong, M. W.; Gonzalez, C.; Pople, J. A. *Gaussian 03*, revision C.02; Gaussian, Inc., Wallingford, CT, 2004 (SN: Pople, PC21390756W-4203N).

Table 1. Crystallographic Data for Compounds **1**−**4**

	1	**2**	**3**	**4**
formula	$C_{28}H_{36}N_8O_{26}Ni_4$	$C_{12}H_{12}N_3O_6Mn$	$C_{48}H_{48}N_{12}O_{20}Mn_6$	$C_{29}H_{24}N_7O_9Cd_2$
fw	1135.49	349.19	1442.62	839.35
crystal system	tetragonal	monoclinic	monoclinic	monoclinic
crystal size, mm	0.30 × 0.20 × 0.20	0.33 × 0.27 × 0.13	0.20 × 0.16 × 0.15	0.20 × 0.20 × 0.20
space group	*P*4(2)/*nnm*	*P*2(1)/*n*	*P*2(1)/*n*	*P*2(1)/*c*
a, Å	14.7651(3)	13.067(3)	16.722(7)	12.615(3)
B, Å	14.7651(3)	8.5169(17)	21.350(8)	12.295(3)
C, Å	8.8902(3)	13.984(3)	16.805(7)	20.242(4)
α, °	90	90	90	90
β, °	90	116.762(2)	102.589(5)	104.1(3)
γ, °	90	90	90	90
V, Å^3	1938.14(9)	1389.6(5)	5856(4)	3044.4(11)
*D*c, Mg m^{-3}	1.946	90	1.636	1.831
Z	2	4	4	4
μ, mm^{-1}	2.2025	0.984	1.338	1.463
reflns collected/unique	9909/958	10 274/3150	39 184/10 286	33 603/6613
	R(int) = 0.0240	*R*(int) = 0.0344	*R*(int) = 0.460	*R*(int) = 0.0266
data/restraints/parameters	958/2/89	3150/0/218	10 286/6/231	6613/3/422
R^a	0.0571	0.0361	0.0933	0.0302
$R_w{}^b$	0.1848	0.1053	0.1627	0.0756
GOF on F^2	1.054	1.138	1.178	1.050
$\Delta\rho_{min}$ and $\Delta\rho_{max}$, e Å^{-3}	−1.037 and −1.036	−0.554 and 0.582	−1.303 and 0.858	−0.911 and 0.923

being 0.2167 Å). The axial positions are occupied by two oxygen atoms (O1 and O1A) from two $HEIDC^{2-}$ ligands. The bond lengths of Ni−O and Ni−N from $HEIDC^{2-}$ are 2.094(4) and 2.075(5) Å, respectively, while the Ni−O distance from water is 2.075(5) Å. The bond angles around each Ni(II) ion vary from 81.25(15) to 179.5(2)°.

In **1**, each Ni(II) ion is coordinated by two N and two O atoms from two separate doubly deprotonated μ_2-$HEIDC^{2-}$ ligands in bis-*N*,*O*-chelating fashion (Scheme 1a), as is found in related octahedral Ni(II) thiocarbohydrazone.[10] Hence, the four Ni(II) are chelated by four μ_2-$HEIDC^{2-}$ ligands forming eight stable five-membered rings. Consequently, four Ni(II) centers are organized as a symmetrical molecular square by four μ_2-$HEIDC^{2-}$ anions. The four Ni atoms are in the same plane (the mean deviation from the plane being 0.000 Å, with a distance of 6.375 Å between adjacent Ni···Ni and with four Ni−Ni−Ni angles of 90°.

Furthermore, complex **1** self-assembles 1D open channel (Figure 1b) along the *c*-axis, which is partially filled with the ethyl from $HEIDC^{2-}$ ligands through intermolecular hydrogen-bonding interactions (Table 3). The weak C−H···OH-bonding also serves as a spring to link the adjacent molecular square blocks to form a 3D network (Figure 1b).

Although several molecular square Ni_4 complexes have been reported,[11] the compound **1** is the first example of a complex having an ideal square planar geometry.

Crystal Structure of Crystalline Polymer {[Mn(HEIDC)-(4,4′-bipy)$_{0.5}$(H$_2$O)]·H$_2$O}$_n$ (2). Complex **2** crystallizes in the monoclinic $P2_1/n$ space group and exhibits a 2D metal-organic framework, which is constructed from alternate 1D left- and right-handed helical chains bridged by 4,4′-bipy.

The asymmetric unit of **2** consists of one Mn(II) ion, one $HEIDC^{2-}$ anion, a half 4,4′-bipy molecule, one coordinated water molecule, and a guest water molecule. As is shown in Figure 2a, each Mn(II) ion is six-coordinated by one nitrogen atom and three oxygen atoms from two individual μ_2-$HEIDC^{2-}$, by one nitrogen atom from a bridging 4,4′-bipy, and by one water molecule showing a slightly distorted octahedral coordination geometry. The Mn−O bond lengths vary from 2.1283(17)−2.2075(17) Å and the Mn−N bond lengths are in the range of 2.231(2)−2.269(2) Å, which are comparable to the previously reported values.[12] The bond angles around each Mn(II) ion vary from 73.66(7) to 174.42(7)°. Each $HEIDC^{2-}$ anion adopts a μ_2-*k*N,O:*k*O, O′ mode (Scheme 1b), and links neighbor Mn(II) ions to form a 1D left-handed helix around the crystallographic 2_1 axis, with the pitches of 8.5169(17) Å, in *b*-axis (Figure 2b). Notably, 4,4′-bipy molecules are parallel within the chains to form a mirror plane (Figure 2c). Therefore, the neighboring chain must be constructed in a left-handed helix to the original formed right-handed chain.[13] Thus, two kinds of parallel helices are bridged by 4,4′-bipy linkages to lead to a novel 2D sheet with (6, 3)-net topology (Figure 2c).

Crystal Structure of Crystalline Polymer [Mn$_6$(EIDC)$_4$-(py)$_4$(H$_2$O)$_4$]$_n$ (3). Single-crystal X-ray analysis has revealed that compound **3** is in the monoclinic $P2_1/n$ space group, as is complex **2**. It displays an interesting 2D sheet structure constructed by $[Mn_3(EIDC)_2]_n$. Mn(II) ions are located in two different coordination environments. As is shown in Figure 3a, Mn(1) is six-coordinated by four oxygen atoms from two individual $EIDC^{3-}$ in the equatorial plane and by two nitrogen atoms from two individual py in axial positions, forming a slightly distorted octahedral geometry. Mn(II) shows a distorted trigonal bipyramidal environment and is five coordinated with two nitrogen atoms from two individual $EIDC^{3-}$ and one oxygen atom from water molecule in the equatorial plane and with two oxygen atoms from two individual $EIDC^{3-}$ in axial positions. The slightly distorted trigonal bipyramidal Mn(III)

(10) (a) Gang, H.; Dong, G.; Duan, C.-Y.; Hong, M.; Meng, Q.-J. *New J. Chem.* **2002**, 1371. (b) Manoj, E.; Kurup, P.; M, R.; Fun, H.-K.; Punnoose, A. *Polyhedron* **2007**, *26*, 4451.

(11) (a) Wasson, A. E.; La Duca, R. L. *Polyhedron* **2007**, *26*, 1001. (b) Mikuriya, M.; Minowa, K.; Nagao, N. *Inorg. Chem. Commun.* **2001**, *4*, 441. (c) Song, X. Y.; Xu, Y. H.; Li, L. C.; Liao, D. Z.; Jiang, Z. H. *Inorg. Chim. Acta* **2007**, *360*, 2039. (d) Mandal, D.; Hong, C. S.; Kim, H. C.; Fun, H. K.; Ray, D. *Polyhedron* **2008**, *27*, 2372. (e) Sung, N. D.; Yun, K. S.; Kim, T. Y.; Choi, K. Y.; Suh, M.; Kim, J. G.; Suh, I. H.; Chin, J. *Inorg. Chem. Commun.* **2001**, *4*, 377.

(12) Lobana, T. S.; Kinoshita, I.; Kimura, K.; Nishioka, T.; Shiomi, D.; Isobe, K. *Eur. J. Inorg. Chem.* **2004**, 356.

(13) (a) Lu, W. G.; Gu, J. Z.; Jiang, L.; Tan, M. Y.; Lu, T. B. *Cryst. Growth Des.* **2008**, *8*, 192. (b) Geng, X. H.; Feng, Y. L.; Lan, Y. Z. *Inorg. Chem. Commun.* **2009**, *12*, 447.

Table 2. Selected Bond Distances (Å) and Angles (°) for Compounds **1**−**4**

1[a]

Ni(1)−N(1)	2.075(5)	Ni(1)−O(1)	2.094(4)
Ni(1)−O(3)	2.075(5)		
N(1)#1−Ni(1)−O(3)	167.30(19)	N(1)−Ni(1)−O(1)	81.25(15)
N(1)#1−Ni(1)−N(1)	96.2(2)	N(1)−Ni(1)−O(3)	89.12(17)
O(3)−Ni(1)−O(3)#1	88.0(3)	N(1)#1−Ni(1)−O(1)	99.10(16)
O(3)−Ni(1)−O(1)	93.08(19)	O(3)#1−Ni(1)−O(1)	86.54(19)
O(1)−Ni(1)−O(1)#1	179.5(2)		

2[b]

Mn(1)−O(3)#1	2.1283(17)	Mn(1)−O(2)#1	2.1657(18)
Mn(1)−O(1)	2.2074(18)	Mn(1)−N(1)	2.232(2)
Mn(1)−O(1W)	2.188(2)	Mn(1)−N(3)	2.269(2)
O(3)#1−Mn(1)−O(2)#1	86.21(7)	O(3)#1−Mn(1)-O(1W)	94.12(7)
O(2)#1−Mn(1)-O(1W)	81.66(7)	O(3)#1−Mn(1)−O(1)	91.27(7)
O(2)#1−Mn(1)−O(1)	97.26(7)	O(1W)−Mn(1)−O(1)	174.42(7)
O(3)#1−Mn(1)−N(1)	163.86(7)	O(2)#1−Mn(1)−N(1)	101.15(7)
O(1W)−Mn(1)−N(1)	101.12(8)	O(1)−Mn(1)−N(1)	73.66(7)
O(3)#1-Mn(1)−N(3)	86.87(8)	O(2)#1−Mn(1)−N(3)	165.45(7)
O(1W)−Mn(1)−N(3)	86.10(8)	O(1)−Mn(1)−N(3)	95.67(7)
N(1)−Mn(1)−N(3)	88.86(8)		

3[c]

Mn(1)−O(3)	2.090(3)	Mn(1)−O(7)#1	2.095(3)
Mn(1)−O(6)#1	2.117(3)	Mn(1)−N(2)	2.296(3)
Mn(1)−O(1)	2.140(3)	Mn(1)−N(1)	2.265(5)
Mn(2)−O(17)	2.110(3)	Mn(2)−O(8)	2.137(3)
Mn(2)−O(2)	2.139(2)	Mn(2)−N(3)	2.162(4)
Mn(2)−N(5)	2.141(4)	Mn(3)−O(18)	2.095(4)
Mn(3)−N(7)	2.134(3)	Mn(3)−O(4)	2.144(3)
Mn(3)−O(9)	2.147(3)	Mn(3)−N(4)	2.149(3)
Mn(4)−O(19)	2.096(3)	Mn(4)−O(14)#2	2.132(3)
Mn(4)−O(12)	2.142(3)	Mn(4)−N(8)	2.153(3)
Mn(4)−N(12)#2	2.169(4)	Mn(5)−O(16)	2.121(3)
Mn(5)−O(11)	2.109(3)	Mn(5)−O(10)	2.117(3)
Mn(5)−O(13)	2.122(3)	Mn(5)−N(9)	2.277(5)
Mn(6)−N(11)	2.155(3)	Mn(6)−N(6)#3	2.134(4)
Mn(6)−O(20)	2.105(3)	Mn(6)−O(5)#3	2.135(3)
Mn(6)−O(15)	2.137(3)	O(6)#1−Mn(1)−O(1)	178.49(11)
O(3)−Mn(1)−O(6)#1	87.02(12)	O(3)−Mn(1)−O(1)	91.61(12)
O(3)−Mn(1)−O(7)#1	179.47(13)	O(7)#1−Mn(1)−O(6)#1	93.50(11)
O(7)#1-Mn(1)−O(1)	87.87(11)	O(6)#1−Mn(1)−O(1)	178.49(11)
N(1)−Mn(1)−N(2)	178.59(15)	O(1)−Mn(1)−N(2)	89.16(11)
O(6)#1−Mn(1)−N(2)	91.46(12)	O(3)−Mn(1)−N(2)	89.46(13)
O(7)#1−Mn(1)−N(2)	90.39(12)	O(1)−Mn(1)−N(1)	91.43(14)
O(6)#1−Mn(1)−N(1)	87.93(15)	O(7)#1−Mn(1)−N(1)	90.91(16)
O(3)−Mn(1)−N(1)	89.24(16)	O(17)−Mn(2)−O(8)	91.05(10)
O(17)−Mn(2)−O(2)	93.74(10)	O(8)−Mn(2)−O(2)	175.19(11)
O(17)−Mn(2)−N(5)	124.34(12)	O(8)−Mn(2)−N(5)	76.64(11)
O(2)−Mn(2)−N(5)	100.18(11)	O(17)−Mn(2)−N(3)	127.12(12)
O(8)−Mn(2)−N(3)	100.16(12)	O(2)−Mn(2)−N(3)	77.30(11)
N(5)−Mn(2)−N(3)	108.52(13)	O(18)−Mn(3)−N(7)	113.94(13)
O(18)−Mn(3)−O(4)	90.51(12)	N(7)−Mn(3)−O(4)	102.49(11)
O(18)−Mn(3)−O(9)	95.37(13)	N(7)−Mn(3)−O(9)	76.35(11)
O(4)−Mn(3)−O(9)	173.96(13)	O(18)−Mn(3)−N(4)	132.79(13)
N(7)−Mn(3)−N(4)	113.20(13)	O(4)−Mn(3)−N(4)	77.07(11)
O(9)−Mn(3)−N(4)	97.85(12)	O(19)−Mn(4)−O(14)#2	96.76(11)
O(19)−Mn(4)−O(12)	92.71(11)	O(14)#2−Mn(4)−O(12)	170.52(11)
O(19)−Mn(4)−N(8)	119.20(12)	O(14)#2−Mn(4)−N(8)	98.68(11)
O(12)−Mn(4)−N(8)	76.82(11)	O(19)−Mn(4)−N(12)#2	121.52(12)
O(14)#2−Mn(4)−N(12)#2	77.21(11)	O(12)−Mn(4)−N(12)#2	97.55(11)
N(8)−Mn(4)−N(12)#2	119.22(13)	O(11)−Mn(5)−O(10)	89.72(11)
O(11)−Mn(5)−O(16)	178.76(12)	O(10)−Mn(5)−O(16)	90.52(11)
O(11)−Mn(5)−O(13)	89.57(11)	O(10)−Mn(5)−O(13)	178.77(12)
O(16)−Mn(5)−O(13)	90.18(11)	O(11)−Mn(5)−N(9)	90.33(13)
O(10)−Mn(5)−N(9)	89.39(15)	O(16)−Mn(5)−N(9)	88.45(13)
O(13)−Mn(5)−N(9)	89.61(15)	O(11)−Mn(5)−N(10)	92.40(11)
O(10)−Mn(5)−N(10)	89.81(12)	O(16)−Mn(5)−N(10)	88.82(12)
O(13)−Mn(5)−N(10)	91.22(12)	N(9)−Mn(5)−N(10)	177.15(14)
O(20)−Mn(6)−N(6)#3	131.88(14)	O(20)−Mn(6)−O(5)#3	94.87(12)
N(6)#3−Mn(6)−O(5)#3	76.47(12)	O(20)−Mn(6)−O(15)	90.91(12)
N(6)#3−Mn(6)−O(15)	99.03(12)	O(5)#3−Mn(6)−O(15)	174.17(13)
O(5)#3−Mn(6)−N(11)	101.05(12)	N(6)#3−Mn(6)−N(11)	115.68(14)
O(20)−Mn(6)−N(11)	112.44(13)	O(15)−Mn(6)−N(11)	77.41(12)

Table 2. Continued

		4[d]	
Cd(1)−N(4)	2.249(2)	Cd(1)−N(1)	2.315(2)
Cd(1)−O(5)	2.350(2)	Cd(1)−N(3)	2.427(3)
Cd(1)−N(6)	2.376(2)	Cd(1)−O(1)	2.391(2)
Cd(2)−N(7)#1	2.297(2)	Cd(2)−N(7)	2.297(2)
Cd(2)−N(2)#2	2.355(2)	Cd(2)−O(7)	2.361(2)
Cd(2)−N(2)#3	2.355(2)	Cd(2)−O(7)#1	2.361(2)
Cd(3)−O(4)#5	2.381(2)	Cd(3)−O(8)#6	2.398(2)
Cd(3)−N(5)#4	2.211(2)	Cd(3)−N(5)#5	2.211(2)
Cd(3)−O(4)#4	2.381(2)	Cd(3)−O(8)	2.398(2)
N(4)−Cd(1)−N(1)	159.40(9)	N(4)−Cd(1)−O(5)	106.67(9)
N(1)−Cd(1)−O(5)	93.88(9)	N(4)−Cd(1)−N(6)	99.12(9)
N(1)−Cd(1)−N(6)	88.60(9)	O(5)−Cd(1)−N(6)	71.34(8)
N(4)−Cd(1)−O(1)	73.07(8)	N(1)−Cd(1)−O(1)	86.55(8)
O(5)−Cd(1)−O(1)	167.84(8)	N(6)−Cd(1)−O(1)	120.82(8)
N(4)−Cd(1)−N(3)	91.05(9)	N(1)−Cd(1)−N(3)	92.90(10)
O(5)−Cd(1)−N(3)	75.20(8)	N(6)−Cd(1)−N(3)	146.53(8)
O(1)−Cd(1)−N(3)	92.63(9)	N(7)#1−Cd(2)−N(7)	180.00(16)
N(7)#1−Cd(2)−N(2)#2	93.24(9)	N(7)−Cd(2)−N(2)#2	86.76(9)
N(7)#1−Cd(2)−N(2)#3	86.76(9)	N(7)−Cd(2)−N(2)#3	93.24(9)
N(2)#2−Cd(2)−N(2)#3	180.00(9)	N(7)#1−Cd(2)−O(7)#1	73.67(8)
N(7)−Cd(2)−O(7)#1	106.33(8)	N(2)#2−Cd(2)−O(7)#1	95.20(8)
N(2)#3−Cd(2)−O(7)#1	84.80(8)	N(7)#1−Cd(2)−O(7)	106.33(8)
N(7)−Cd(2)−O(7)	73.67(8)	N(2)#2−Cd(2)−O(7)	84.80(8)
N(2)#3−Cd(2)−O(7)	95.20(8)	O(7)#1−Cd(2)−O(7)	180.00(16)
N(5)#4−Cd(3)−N(5)#5	180.00(16)	N(5)#4−Cd(3)−O(4)#5	105.98(8)
N(5)#5−Cd(3)−O(4)#5	74.02(8)	N(5)#4−Cd(3)−O(4)#4	74.02(8)
N(5)#5−Cd(3)−O(4)#4	105.98(8)	O(4)#5−Cd(3)−O(4)#4	180.00(10)
N(5)#4−Cd(3)−O(8)	88.04(9)	N(5)#5−Cd(3)−O(8)	91.96(9)
O(4)#5−Cd(3)−O(8)	88.04(8)	O(4)#4−Cd(3)−O(8)	91.96(8)
N(5)#4−Cd(3)−O(8)#6	91.96(9)	N(5)#5−Cd(3)−O(8)#6	88.04(9)
O(4)#5−Cd(3)−O(8)#6	91.96(8)	O(4)#4−Cd(3)−O(8)#6	88.04(8)
O(8)−Cd(3)−O(8)#6	180.00(9)		

Symmetry transformations used to generate equivalent atoms: [a] #1: $x, -y+3/2, -z+1/2$. [b] #1: $-x+3/2, y+1/2$. [c] #1: $x+1/2, -y-1/2, z+1/2$; #2: $x+1/2, -y-3/2, z+1/2$; #3: $x-1/2, -y-1/2, z-1/2$. [d] #1: $-x, -y, -z$; #2: $x-1, y, z$; #3: $-x+1, -y, -z$; #4: $x, -y+1/2, z-1/2$; #5: $-x, y+1/2, -z+1/2$; #6: $-x, -y+1, -z$.

atom has in its pseudoequatorial plane the oxygen atom O18 (from the coordinated water molecule) and two nitrogen atoms N4 and N7 from two $EIDC^{3-}$ units; the oxygen atoms O4 and O9 (from the two $EIDC^{3-}$ units) occupy the pseudoaxial sites. The Mn−O bond lengths vary from 2.090(3)−2.147(3) Å and the Mn−N bond lengths fall in the range of 2.134(3)−2.296(3) Å. The Mn−O bond distances are slightly shorter than those of complex **2**. The coordination environments of Mn(II) atoms are similar to those of Zn(II) atoms in a recent reported compound with the similar ligand H_3IDC, $\{[Zn_3(IDC)_2(bpy)_3]\cdot(bpy)\cdot 8H_2O\}_n$.[14]

In **3**, each $EIDC^{3-}$ anion adopts a μ_3-*k*N,O:*k*O,O′:*k*N′, O′ mode (Scheme 1c) to bridge three Mn(II) ions in *N*,*O*-chelating, *O*,*O*′-chelating, and *N*′,*O*′-chelating. The overall structure of **3** is a 2D honeycomb-like sheet of $[Mn_3(EIDC)_2]_n$ containing infinite 24-membered rings (Figure 3b). Each 24-membered ring forms a hexagon and is formed by six μ_3-$EIDC^{3-}$ anions, two octahedral Mn(II), and four trigonal bipyramidal Mn(II) cations. The honeycomb-like sheet of **3** is similar to the structural motifs of $[Zn_3(IDC)_2]_n$ and $[Co_3(IDC)_2]_n$ in compounds $\{[Zn_3(IDC)_2(bpy)_3]\cdot(bpy)\cdot 8H_2O\}_n$[14] and $\{[Co_3(IDC)_2(bpy)_3)]\cdot 6H_2O\cdot DMF\}_n$, respectively.[15]

Crystal Structure of Crystalline Polymer $\{[Cd_2(EIDC)(H_2EIDC)(4,4'\text{-bipy})_{1.5}]\cdot H_2O\}_n$ (4). Complex **4** crystallizes in the monoclinic space group $P2(1)/c$, which is assembled in a 3D framework with three Cd(II) atoms, one and a half 4,4′-bipy molecules, one $EIDC^{3-}$ anion, and one H_2EIDC^- anion in each asymmetric unit.

The three crystallographically independent Cd(II) ions (Figure 4a) exhibit different coordination environments. Cd(I) is six-coordinated with two oxygen (O1, O5) and two nitrogen (N4, N6) atoms from two individual μ_3-$EIDC^{3-}$ and μ_2-H_2EIDC^-, and two nitrogen (N1, N3) atoms from two individual 4,4′-bipy molecules. Cd(II) is six-coordinated with two oxygen (O7A, O7) and two nitrogen (N7A, N7) atoms from two individual μ_3-$EIDC^{3-}$ in the equatorial plane and with two nitrogen (N2B, N2C) atoms from two individual 4,4′-bipy molecules in axial positions. Cd(III) is six-coordinated with four oxygen (O4D, O4E, O8, O8F) and two nitrogen (N5D, N5E) atoms from two individual μ_3-$EIDC^{3-}$ and two individual μ_2-H_2EIDC^-. The Cd−O bond distances ranging from 2.350(2) to 2.398(2) Å and Cd−N bond distances varying from 2.11(2) to 2.427(3) Å are consistent with the previously reported values.[16] Obviously, in **4**, all metal sites exhibit octahedronal coordination geometry.

Interestingly, singly deprotonated H_2EIDC^- and triply deprotonated $EIDC^{3-}$ coexist in **4**, and they adopt two types of coordination modes, namely μ_2-*k*N, O:*k*N′,O′ (Scheme 1d), and μ_3-*k*N, O:*k*O:*k*N′,O′ (Scheme 1e). As is shown in Figure 4b, each $EIDC^{3-}$ anion bridges three Cd(II) atoms in *N*,*O*-chelating, *O*-bridging, and *N*′,*O*′-chelating coordination modes to form a 1D infinite chain

(14) Lu, W. G.; Jiang, L.; Feng, X. L.; Lu, T. B. *Cryst. Growth Des.* **2006**, *6*, 564.

(15) Wang, Y. L.; Yuan, D. Q; Bi, W. H; Li, X.; Li, X. J.; Li, F.; Cao, R. *Cryst. Growth Des.* **2005**, *5*, 1849.

(16) Lu, W. G.; Jiang, L.; Feng, X. L.; Lu, T. B. *Cryst. Growth Des.* **2008**, *8*, 986.

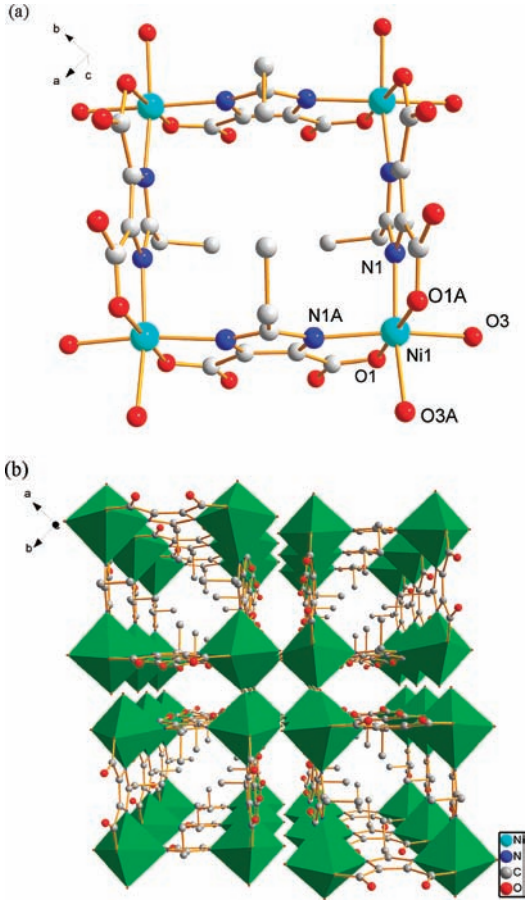

Figure 1. (a) Molecular square structure of the tetranuclear Ni(II) complex **1** (hydrogen atoms and solvent molecules omitted for clarity). (b) A 3D solid-state network of **1** constructed by intermolecular hydrogen-bonding interactions containing 1D open channels along the *c*-axis.

Table 3. Hydrogen Bond Distances (Å) and Angles (°) for **1**[a]

D−H···A	d(H···A)	d(D···A)	∠(DHA)
O(2)−H(2A)···O(2)#2	1.264(15)	2.496(7)	162(8)
O(3)−H(3W2)···O(2)#3	1.966(18)	2.808(6)	171(9)
O(3)−H(3W1)···O(3)#4	2.09(4)	2.890(10)	158(9)

[a]Symmetry transformations used to generate equivalent atoms: #2: $y + 1/2, x - 1/2, z$; #3: $-y + 3/2, -x + 3/2, -z$; #4: $-x + 3/2, y, -z + 1/2$.

(Figure 4b) with the Cd2···Cd3 distance of 6.1473(12) Å along the *b*-axis. Furthermore, the 1D infinite chains are linked to a 2D layer by bridging 4,4′-bipy (Figure 4c). It is noteworthy that adjacent layers are pillared by μ_2-H_2EIDC^- ligands in *N*,*O*-chelating and *N*′,*O*′-chelating coordination modes. Finally, the μ_2-4,4′-bipy bridge can pass through the adjacent layer to connect two layers to result in an interpenetrating 3D framework (Figure 4d).

Synthesis and Characterization. As is aforementioned in the Introduction Section, the factors governing the reaction and formation of the hydrothermal product are complicated. The position and type of functional groups on the ligands are crucial for the generation of supramolecular frameworks. In order to predict the ethyl substituent effect in our ligand, H_3EIDC, the optimized geometries and the Mulliken atomic charge distributions of the free ligand H_3EIDC and the related ligand H_3IDC have been calculated by the B3LYP/6-311++G(d, p) level of theory. The computed results (Scheme 2 and Table 4) reveal that the free ligands H_3EIDC and H_3IDC have two features: (i) The negative Mulliken atomic charges mainly distribute on the oxygen and nitrogen atoms. The Mulliken charges are −0.66499 for O1, −0.65854 for O2, −0.68904 for O3, −0.64712 for O4, −0.52367 for N5, and −0.49327 for N6 in the free ligand H_3IDC, and −0.66617 for O1, −0.66085 for O6, −0.69129 for O2, −0.65133 for O13, −0.53170 for N7, and −0.49906 for N6 in the free ligand H_3EIDC (Table 4). These values indicate that the oxygen and nitrogen atoms of the two ligands all have potential ability of coordinating to metal ions. So H_3IDC and H_3EIDC can show various coordination modes under appropriate reaction conditions. This finding can be confirmed by both previous[5,6] and our present experimental results. It is also interesting to compare the coordination modes of the $H_{3-n}EIDC^{n-}$ species in **1**−**4**. In **1**, the imidazole−*H* and COO−*H* are removed from the ligand H_3EIDC to form the $HEIDC^{2-}$ unit. Two COO−*H* are deprotonated in **2** also leading to the $HEIDC^{2-}$ unit. The triply deprotonated $EIDC^{3-}$ units can be found in **3**. In **4**, there are two different deprotonated forms, H_2EIDC^- (imidazole−H removed) and $EIDC^{3-}$ (triply deprotonated). (ii) Compared with the free ligand H_3IDC, the introduction of ethyl group into H_3EIDC has some effect on the Mulliken charge distributions of the oxygen and nitrogen atoms. As is discussed above, the Mulliken charge distributions of oxygen and nitrogen atoms in H_3EIDC all increase slightly, which shows that the coordination abilities of these atoms may be enhanced, especially of O13, O6, and O7 atoms. However, the substituent electronic effect of the ethyl unit in the ligand H_3EIDC is not remarkable. This can be further confirmed by calculating the highest occupied molecular orbital (HOMO) distributions of the free ligands H_3IDC and H_3EIDC (see Supporting Information, Figure S1). It can be seen from the figure S1, that the electron density of the HOMO in H_3EIDC has no significant change in comparison with the H_3IDC. Therefore, the steric effect of the ethyl unit in H_3EIDC should be given more consideration. When H_3IDC or H_3EIDC react with $Ni(NO_3)_2$ under similar solvent $EtOH/H_2O$ and temperature conditions, two different structural complexes, octanuclear complex $[Ni_8(H_2IDC)_8(HIDC)_4]\cdot 8EtOH\cdot 18H_2O$[5q] and tetranuclear complex **1** are produced. Obviously, the steric hindrance of the ethyl group may hold the H_2EIDC^- to link more Ni(II) ions.

The stoichiometry of the starting materials is important for the formations of complexes **1**−**4**. The reactions of metal salts and H_3EIDC in a molar ratio of 1:1, 1:1, 1:1, and 1:1 have respectively produced the crystals of **1**−**4** successfully, while other stoichiometry has failed to produce suitable crystals or has given products with low yields (about 1.5%).

It is to be pointed out that complex **1** has been obtained with high yield by the solvothermal reaction of $Ni(NO_3)_2$ and H_3EIDC in an $EtOH-H_2O$ (6:1) mixed solution. In the preparation of **1**, the change in organic solvent or the adoption of hydrothermal synthesis cannot result in any crystalline products of **1**, but some unidentified powder. The results indicate that the forming of the framework of **1** is considerably influenced by the nature of the solution. In addition, we have also attempted to replace the Ni(II) with Mn(II) in the synthesis of **2**, only leading to the formation of a mononuclear complex $[Mn(H_2EIDC)_2(H_2O)_2]\cdot 3H_2O$ (Supporting Information, Figure S2) rather than an Mn(II) analogue of **1**. This fact also implies

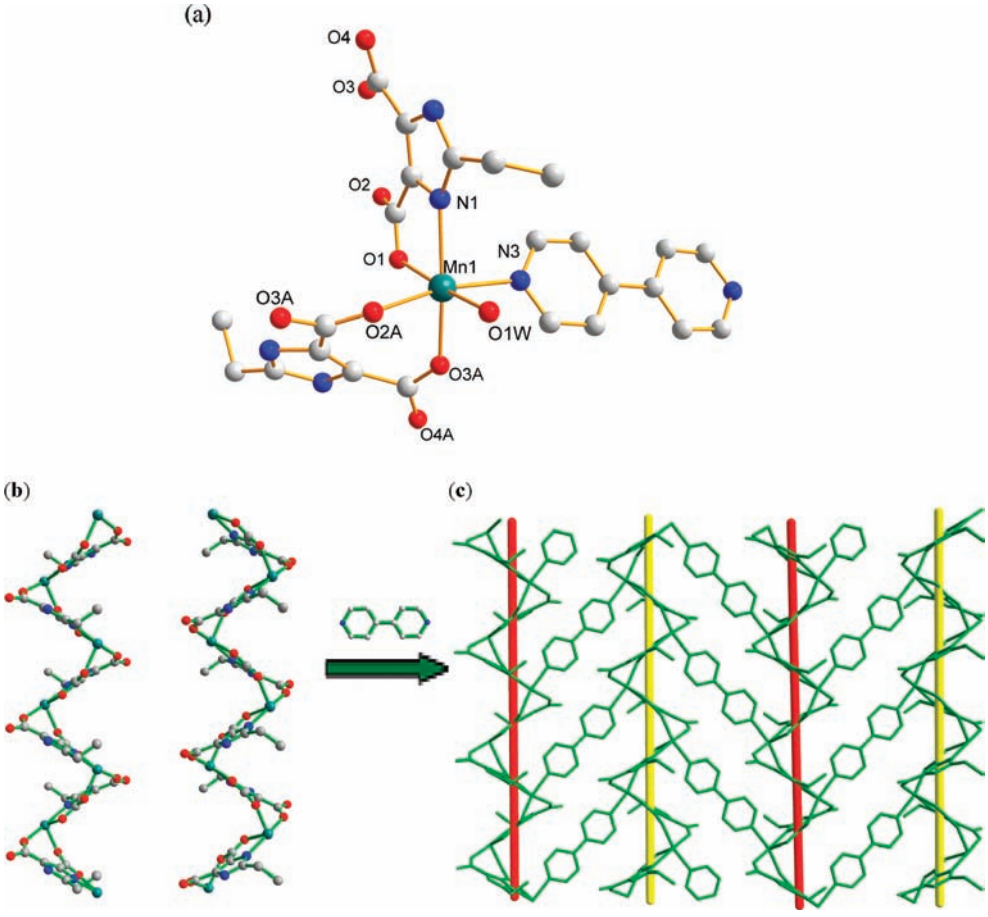

Figure 2. (a) Coordination arrangements of the Mn(II) in complex **2** (hydrogen atoms and solvent molecules omitted for clarity). (b) The 1D left-handed helical chain of $[Mn(HEIDC)]_n$ and 1D right-handed helical chain of $Mn(HEIDC)]_n$ around the 2_1 axis. (c) The 2D sheet comprising infinite helical chains bridged by 4,4′-bipy linkages.

that the formation of tetranuclear structure in **1** is metal ion dependent.

The selection of coligands in the synthesis process of complexes **1**−**4** has been based on two aspects, as follows: First, the coligands sometimes play important roles in directing the extended structure of the resulting complex.[5] When we use 4,4′-bipy as auxiliary ligands, one novel 2D framework **2** and one 3D polymer **4** have been prepared. Second, during the reactions, some coligands such as prz (piperazine)[13a] or py have served not only as an auxiliary ligand but also as a deprotonated agent due to its strong alkalinity. In the preparation of **3** or **4**, py has been adopted mainly to adjust pH values; also it can coordinate to the central metal ions and benefit the crystallization of polymer **3**.

The selection of the appropriate multidentate ligand to link paramagnetic metal ions is a powerful way for the building of molecular magnetic materials. Ni(II) and Mn(II) ions are good candidates, which can be linked by carboxylate or N-containing ligands to form extended coordination networks allowing for sufficiently strong magnetic exchange. The Cd(II) cation is able to coordinate simultaneously to both O- and N-containing ligands to obtain intriguing architectures. Thus, Ni(II), Mn(II), and Cd(II) ions are selected by us to react with H_3EIDC in the presence of (or without) coligands. It is noteworthy that the anion of metal salt may affect the crystal shape of the final product. If the $Ni(NO_3)_2$ is changed to $Ni(OAc)_2$ or $NiSO_4$ in the synthesis of **1**, then only a small crystalline powder can be generated, which suggests that the anion NO_3^- plays an important role in the formation of **1**. The similar cases can be found in the syntheses of **2**−**4**. However, the anion effect in the construction of coordination complexes is ambiguous.

In conclusion, by fine control over synthetic conditions such as solvent, pH values, metal/ligand molar ratio, and coligands the reproducibility of our experiments is good.

The IR spectra display characteristic absorption bands for water molecules, carboxylate, imidazolyl units and pyridyl units. Compounds **1**−**4** show strong and broad absorption bands in the range of 3400−3500 cm^{-1}, which indicates the presence of hydrogen-bonded water molecules. The coordination of the carboxylate can be seen from the absorption bands in the frequency range 1340−1610 cm^{-1} in **1**−**4** due to $\nu_{as}(COO^-)$ and $\nu_s(COO^-)$ vibrations respectively. The strong bands in the range of 1610−1570 cm^{-1} in complexes **1**−**4** imply the C═N and C═C stetching bands of imidazole ring in H_3EIDC.

Compounds **1**−**3** show similar thermal behaviors, but are different from **4**. The TG curves for **1**−**4** are shown in Figure 5, and the DSC curves for **1**−**4** are illustrated in (Supporting Information, Figure S3).

There are two small endothermic peaks at 184.0 and 283.9 °C and one very strong exothermic peak at 423.0 °C on the DSC curve of polymer **1**. The first weight loss of 2.2% (calculated 1.6%) occurs at about 150 °C, which is attributed to the loss of free water molecules. The second weight loss of 72.30% between 250 and 460 °C corre-

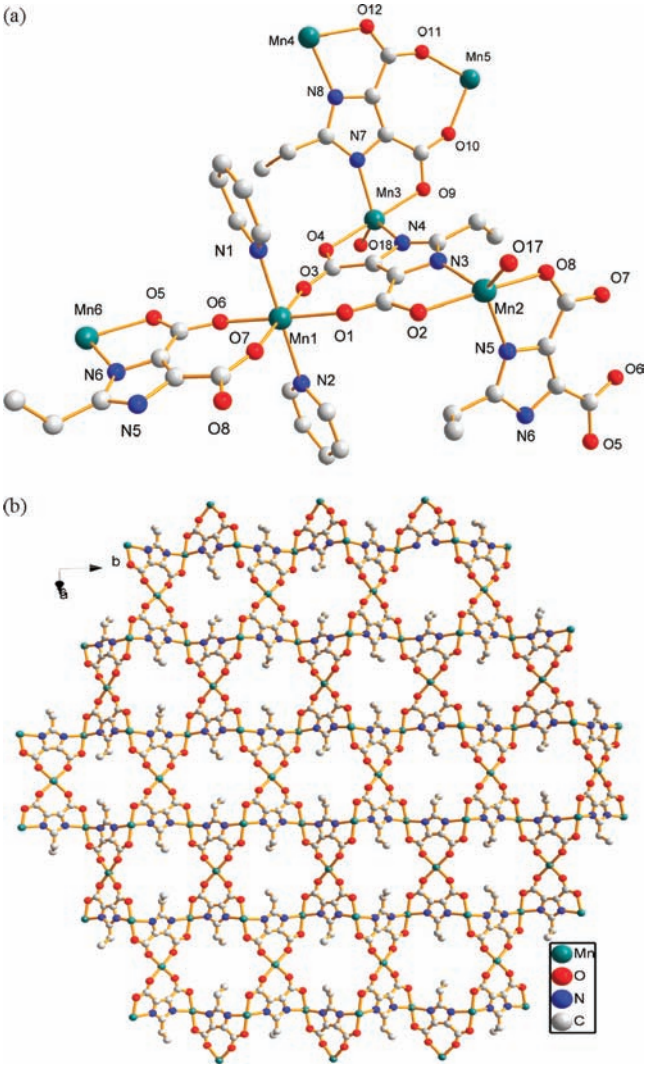

Figure 3. (a) Coordination environments of Mn(II) atom in polymer **3** (hydrogen atoms omitted for clarity). (b) The 2D honeycomb-like with 24-membered hexagonal rings (pyridine and coordinated water molecules omitted for clarity).

sponds to the loss of coordinated water molecules and $HEIDC^{2-}$. The remaining weight of 25.1% corresponds to the percentage (calculated 25.6%) of the Ni and O components, indicating that the final product is 4NiO.

The TG−DSC curves have been obtained under flowing air for a crystalline sample of **2** in the temperature range of 20−800 °C. TG data show that polymer **2** is stable up to 169.9 °C then loses weight from 169.9 to 254.9 °C (observed 10.43%, calculated 10.25%), corresponding to losses of both solvent water and coordinated water molecules. Subsequently, a plateau region is observed from 204.2 to 254.9 °C. It keeps losing weight from 254.9 to 367.3 °C corresponding to the decomposition of 4,4′-bipy and $HEIDC^{2-}$ units (observed 23.50%, calculated 22.88%). A white amorphous residue is MnO (observed 21.11%, calculated 20.20%). One very strong exothermic peak at 463.3 °C can be observed on the DSC curve of polymer **2**.

For polymer **3**, there is one weak endothermic peak (213.5 °C), one weak exothermic peak (335.1 °C), and one strong exothermic peak (408.6 °C) in the DSC curve. It loses coordinated water molecules in the temperature range of 110−210 °C (observed 5.7%, calculated 6.3%). It keeps losing weight from 240 to 465 °C, corresponding to the decomposition of the $EIDC^{3-}$ and py (observed 62.3%, calculated 62.2%). The decomposed reactions end at 561.5 °C. The final residue is 6MnO (observed 32.0%, calculated 31.5%).

There are two strong exothermic peaks at 401.2 and 521.7 °C on the DSC curve of compound **4**. It first loses the crystallized water molecules in the temperature range of 41−157 °C (observed 2.8%, calculated 2.1%), and second loses weight from 332 to 524 °C corresponding to the decomposition of 4,4′-bipy and H_2EIDC^{2-} and $EIDC^{3-}$ units (observed 67.5%). Finally, a plateau region is observed from 524 to 800 °C. A white amorphous residue is 2CdO (observed 29.7%, calculated 30.5%).

In conclusion, the IR data and thermal data of complexes **1**−**4** are in reasonable agreement with the crystal structure analysis.

Magnetic Properties. **Polymer 1**: Variable-temperature magnetic study on **1** is carried out over the temperature range of 2.0−300 K. The variation of the inverse of the magnetic susceptibility, χ_m^{-1} and $\chi_m T$ of **1** are shown in Figure 6a. The thermal evolution of χ_M^{-1} obeys the Curie−Weiss law, $\chi_M = C/(T - \theta)$ in the temperature range of 60−300 K with Weiss constant, θ, of −48.69 K and Curie constant, C_M, of 5.170 cm^3 K mol^{-1}. It can be seen from Figure 6a, at 300 K, $\chi_M T$ is equal to 4.450 cm^3 K mol^{-1} and is slightly below the spin-only value of four uncoupled ($S_{Ni} = 1$, $g = 2.20$) nickel(II) ions (4.83 cm^3 K mol^{-1}).[17] As the temperature is lowered, the $\chi_M T$ value steadily decreases to 0.143 cm^3 K mol^{-1} at 2.0 K. Such behavior can be referred to as the presence of an antiferromagnetic exchange behavior between the neighbor Ni(II) ions.

As is shown in the crystallographic part, the complex **1** is made up of Ni_4 entities where the ligand $HEIDC^{2-}$ acts as a bridge to afford a square system (Figure 1a). Obviously, we can expect that the magnetic pathways between the two neighbor Ni(II) ions are the same in polymer **1**. That is to say, the four Ni(II)−HEIDC−Ni(II) couplings are equal. Taking into account this fact, we can use a single coupling constant J. Thus, for a square arrangement of four metal centers, a D_{4h} [2 × 2] grid, the spin Hamiltonian of the form of eq 1 can be used to describe the magnetic properties of the compound with $S = 1$:

$$\hat{H} = -2J(\hat{S}_1\hat{S}_2 + \hat{S}_2\hat{S}_3 + \hat{S}_3\hat{S}_4 + \hat{S}_4\hat{S}_1) \qquad (1)$$

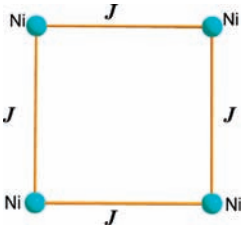

The allowed eigenvalues were then substituted into the following modified equation:[18]

$$\chi_M = \frac{Ng^2\beta^2}{3kT}\frac{A}{B}\rho + \frac{Ng^2\beta^2}{3kT}(1-\rho) + TIP$$

(17) Demeshko, S.; Leibeling, G.; Dechert, S.; Meyer, F. *Dalton Trans.* **2006**, 3458.
(18) Kahn, O. *Molecular Magnetism*; VCH: New York, 1993.

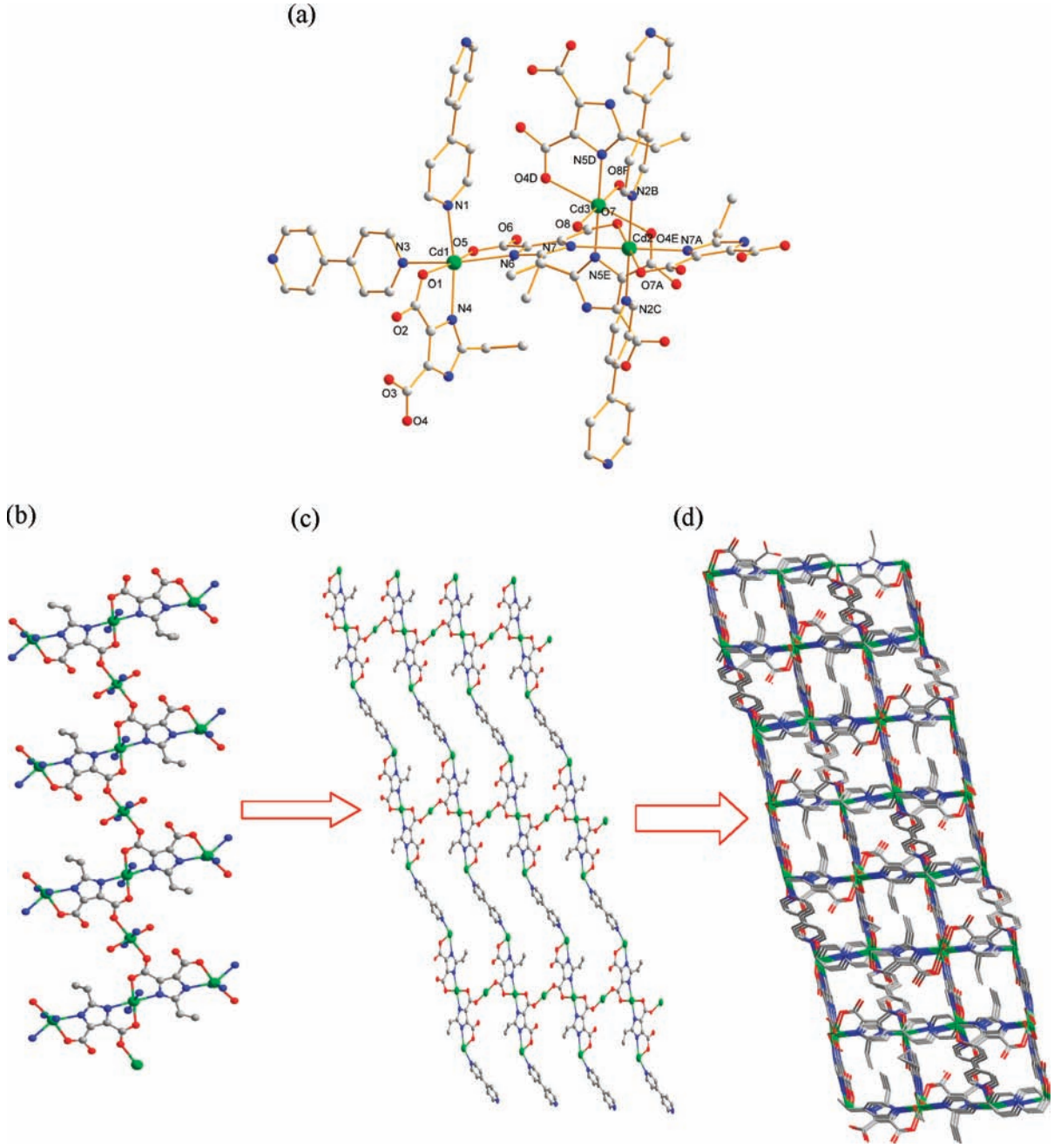

Figure 4. (a) The segment of polymer **4**, showing the local coordination environments of Cd(II) ions (hydrogen atoms and solvent molecules omitted for clarity). (b) 1D chain along the *b*-axis based on Cd(II) and μ_3-EIDC^{3-}. (c) 2D layer constructed from μ_3-EIDC^{3-} (Scheme 1e) and 4,4′-bipy. (d) 3D framework along the *a*-axis built by 2D layers, μ_2-HEIDC^{2-} (Scheme 1d) and 4,4′-bipy (hydrogen atoms and solvent molecules omitted for clarity).

where $A = 108 + 6\exp(18a) + 42\exp(14a) + 66\exp(10a) + 256\exp(8a) + 30\exp(6a) + 168\exp(4a)$; $B = 90 + \exp(20a) + 3\exp(18a) + 11\exp(14a) + \exp(12a) + 13\exp(10a) + 24\exp(8a) + 5\exp(6a) + 14\exp(4a)$; $a = -J/kT$. Other parameters of N, β, K, g, TIP, and T have their usual meanings, while ρ is the fraction of paramagnetic impurity.

The best fitting for the data in the range of 2−300 K gives $J = -10.83$ cm^{-1}, $g = 2.19$, $\rho = 0.0433$, TIP = 0.00569 cm^3 mol^{-1}, with $R = 5.2 \times 10^{-4}$, [$R = [\sum(\chi_{obs} - \chi_{calc})^2/\sum\chi_{obs}]^{1/2}$].

Although there are some reports about magnetic properties of tetranuclear Ni(II) complexes,[19] the studies of magnetic properties concerning molecular square built by four Ni(II) ions are rare.[10,17,20] Indeed, only several examples can be found in the references. For example, Arora and co-workers have reported the ferromagnetic exchange interaction ($J = 1.0$ cm^{-1}) mediated by syn−anti carboxylate bridging of an approximately square planar complex {[Ni^{II}(L^1)][ClO$_4$]}$_4$·CH$_3$CN (L^1(−) = 3-[*N*-methyl-{2-(pyridine-2-yl)ethyl}amino]propionate).[20a] Moroz and co-workers have studied the antiferromagnetic interaction of [2 × 2] molecular grid nickel(II) complex [Ni$_4$(**pop**)$_4$(HCOO)$_4$]·7H$_2$O[20b] (H**pop** = 2-hydroxyimino-*N*′-[1-(2-pyridyl)ethylidene]propanohydrazone) with a new polydentate oxime-containing Schiff base ligand and have fitted the magnetic parameter of the complex ($J = -14.7(1)$ cm^{-1}). Meng and co-workers have described the antiferromagnetic coupling among the Ni(II) ions of two similar approximately square

Scheme 2. The Optimized Geometries of the Free Ligands H_3IDC and H_3EIDC[a]

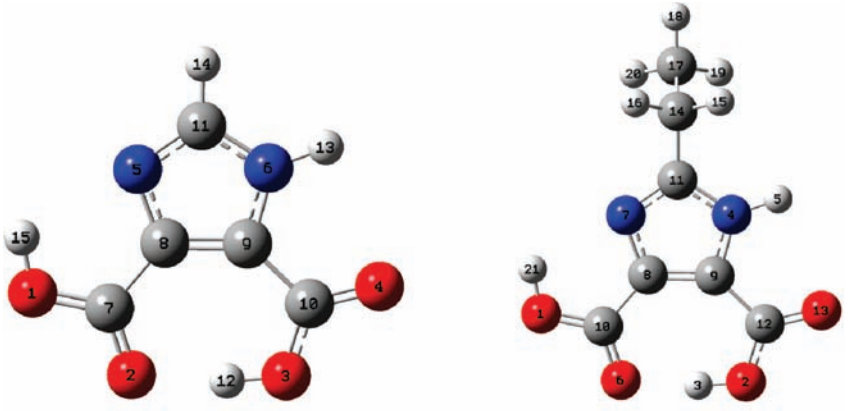

[a] The blue ball represents N atom, the red ball represents O atom and the gray ball represents C atom.

Table 4. Mulliken Atomic Charge Distributions of the Free Ligands H_3EIDC and H_3IDC

H_3IDC		H_3EIDC	
atom number	Mulliken charge	atom number	Mulliken charge
O1	−0.66499	O1	−0.66617
O2	−0.65854	O6	−0.66085
O3	−0.68904	O2	−0.69129
O4	−0.64712	O13	−0.65133
N5	−0.52367	N7	−0.53170
N6	−0.49327	N4	−0.49906
C7	0.80744	C10	0.80683
C8	0.01044	C8	0.01558
C9	0.05658	C9	0.05461
C10	0.78105	C12	0.77963
C11	0.24933	C11	0.44052
H12	0.50665	C14	−0.43529
H13	0.48765	C17	−0.56473
H14	0.23673	H15	0.22625
H15	0.54074	H16	0.23251
		H18	0.20938
		H19	0.20176
		H20	0.20415
		H21	0.54017

planar complexes $[Ni(HL^2)]_4[PF_6]_4$[10a] (H_2L^2 = bis(2-acetylpyridine)thiocarbazone) and $[Ni(HL^3)]_4[PF_6]_4 \cdot 4EtOH \cdot H_2O$[20c] ($H_2L^3$ = bis[phenyl(2-pyridyl)thiocarbazone), not given the theoretically fitted J value. Compared with the strong antiferromagnetic coupling interactions of the previous molecular square Ni(II) $[Ni(HL^4)]_4[PF_6]_4 \cdot 0.5EtOH \cdot 2.8H_2O$[20c] ($H_2L^4$ = bis(2-pyridyl ketone)thiocarbohydrazone), the J value of our complex is relatively low, which is close to the value of the complex $[Ni_4(\mathbf{pop})_4(HCOO)_4] \cdot 7H_2O$.[20b] Obvious, this is due to the long Ni···Ni separation (6.375 Å) and the complicated pathway by the ligand $HEIDC^{2-}$.

Polymer 2: Variable-temperature magnetic susceptibility of **2** is measured in the 2.0−300 K temperature range. The variation of the inverse of the magnetic susceptibility, χ_M^{-1} and $\chi_M T$ of **2** are shown in Figure 6b. The thermal evolution of χ_M^{-1} obeys the Curie−Weiss law, $\chi_M = C/(T - \theta)$ in the range of 6.8−300 K with a Weiss constant, θ, of −10.438 K and a Curie constant, C_M, of 4.478 cm^3 K mol^{-1}, respectively. At 300 K, the $\chi_M T$ value is 4.301 cm^3 K mol^{-1} (5.86 μB), which is close to the value of 4.38 cm^3 K mol^{-1} (5.92 μB) expected for magnetically isolated high-spin Mn(II) (S_{Mn} = 5/2, g = 2.0) and is near the reported polymers $(H_2NMe_2)[Mn(tzdc)] \cdot 0.5H_2O$ (tzdc = 1,2,3-trizole-4,5-dicarboxylate) (4.31 cm^3 K mol^{-1})[21] and $[Mn_2(btr)(\mu\text{-}ox)_2(H_2O)] \cdot 2H_2O$ (btr = 4,4′-bis-1,2,4-triazole, ox = oxalate anion) (4.32 cm^3 K mol^{-1})[22] in the literature. On lowering the temperature, the $\chi_M T$ value decreases smoothly, and below 47 K it decreases abruptly to a minimum of 0.409 cm^3 K mol^{-1} at 2 K. The negative θ value and the $\chi_M T$ vs T curve reveal typical antiferromagnetic interactions between the Mn(II) centers in polymer **2**.

According to the structural data, the μ_2-$HEIDC^{2-}$ units link the Mn(II) ions into infinite chains. Hence the 2D layer has been constructed by 4,4′-bipy bridging these chains. Obviously, there are two pathways to transmit the magnetic interactions: μ_2-HEIDC- and 4,4′-bipy-bridge, whereas the super exchange interactions between Mn(II)

(19) (a) Efthymiou, C. G.; Papatriantafyllopoulou, C.; Alexopoulou, N. I.; Raptopoulou, C. P.; Boča, R.; Mrozinski, J.; Bakalbassis, E. G.; Perlepes, S. P. *Polyhedron* **2009**, *28*, 3373. (b) Biswas, B.; Pieper, U.; Weyhermuller, T.; Chaudhuri, P. *Inorg. Chem.* **2009**, *48*, 6781. (c) Manca, G.; Cano, J.; Ruiz, E. *Inorg. Chem.* **2009**, *48*, 3139. (d) Ran, J. W.; Zhang, S. Y.; Xu, B.; Xia, Y. Z.; Guo, D.; Zhang, J. Y.; Li, Y. H. *Inorg. Chem. Commun.* **2008**, *11*, 73. (e) Aromí, G.; Bouwman, E.; Burzurí, E.; Carbonera, C.; Krzystek, J.; Luis, F.; Schlegel, C.; van Slageren, J.; Tanase, S.; Tea, S. J. *Chem.—Eur. J.* **2008**, *14*, 11158. (f) Moragues-Canovas, M.; Helliwell, M.; Ricard, L.; Riviere, E.; Wernsdorfer, W.; Brechin, E.; Mallah, T. *Eur. J. Inorg. Chem.* **2004**, 2219. (g) Pavlishchuk, V. V.; Kolotilov, S. V.; Addison, A. W.; Prushan, M. J.; Schollmeyer, D.; Thompson, L. K.; Weyhermuller, T.; Goreshnik, E. A. *Dalton Trans.* **2003**, 1587. (h) Mikuriya, M.; Tanaka, K.; Inoue, N.; Yoshioka, D.; Lim, J. W. *Chem. Lett.* **2003**, *32*, 126. (i) Du, M.; Bu, X.-H.; Guo, Y.-M.; Zhang, L.; Liao, D.-Z.; Ribas, J. *Chem. Commun.* **2002**, 1478. (j) Pavlishchuk, V. V.; Kolotilov, S. V.; Addison, A. W.; Prushan, M. J.; Schollmeyer, D.; Thompson, L. K.; Goreshnik, E. A. *Angew. Chem., Int. Ed., Engl.* **2001**, *40*, 4734. (k) Clemente-Juan, J. M.; Chansou, B.; Donnadieu, B.; Tuchagues, J. P. *Inorg. Chem.* **2000**, *39*, 5515. (l) Saalfrank, R. W.; Trummer, S.; Reimann, U.; Chowdhry, M. M.; Hampel, F.; Waldmann, O. *Angew. Chem., Int. Ed., Engl.* **2000**, *39*, 3492. (m) Fallah, M. S. E.; Rentschler, E.; Caneschi, A.; Gatteschi, D. *Inorg. Chim. Acta* **1996**, *247*, 231.

(20) (a) Arora, H.; Lloret, F.; Mukherjee, R. *Dalton Trans.* **2009**, 9759. (b) Moroz, Y. S.; Kulon, K.; Haukka, M.; Gumienna-Kontecka, E.; Kozlowski, H.; Meyer, F.; Fritsky, I. O. *Inorg. Chem.* **2008**, *47*, 5656. (c) He, C.; Duan, C.-Y.; Fang, C.-J.; Liu, Y. J.; Meng, Q.-J. *J. Chem. Soc., Dalton Trans.* **2000**, 1207.

(21) Zhang, W. X.; Xue, W.; Li, J. B.; Zheng, Y. Z.; Chen, X. M. *CrystEngComm* **2008**, *10*, 1770.

(22) Huang, Y. Q.; Cheng, P. *Inorg. Chem. Commun.* **2008**, *11*, 66.

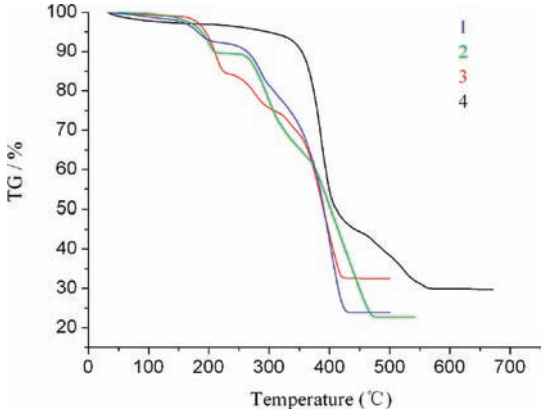

Figure 5. The TGA curves for complexes **1**−**4**.

ions by the 4,4′-bipy-bridge can be ignored because of the long length of 4,4′-bipy ligands. On the other hand, until now, no appropriate theory model has been established to determine the magnetic coupling constant between metal ions for a 2D layer polymeric complex. In order to evaluate the magnetic interactions in **2**, we employ an approximate approach that has been used for similar cases.[22,23] The magnetic susceptibility of **2** has been fitted to the Fisher model[24] of the isotropic Heisenberg antiferromagnet, and later modified by Wagner and Friedberg[25] for a Mn^{2+} system of spin 5/2 which is

$$\chi = \frac{Ng^2\beta^2 S(S+1)}{3KT}\frac{1+u}{1-u}$$

where u is the well-known Langevin function defined as $u = \coth[JS(S+1)/kT] - kT/[JS(S+1)]$ with $g = 2.0$, $S = 5/2$ for Mn(II), and N, β, K, g, and T have their usual meanings. Due to further assembly of the 1D chains into a 2D MOF, the fit function can be modified to include the interchain coupling.[26] The function, therefore, is

$$\chi_M = \frac{\chi}{1-(2zJ'/Ng^2\beta^2)\chi}$$

where J' is the interchain exchange coupling constant and z is the number of the nearest neighbor chains. The best fitting for the data in the range of 2−300 K gives $J = -0.025\ cm^{-1}$, $zJ' = -0.02\ cm^{-1}$, and $g = 2.0$, with $R = 3.5\times 10^{-4}$, [$R = [\sum(\chi_{obs} - \chi_{calc})^2/\sum\chi_{obs}]^{1/2}$]. The negative coupling constant J confirms the existence of an antiferromagnetic exchange within in polymer **2**.

Polymer 3: Variable-temperature magnetic study on **3** is performed over the temperature range of 2.0−300 K. The variation of the inverse of the magnetic susceptibility, χ_M^{-1} and $\chi_M T$ of **3** are shown in Figure 6c. The thermal evolution of χ_M^{-1} obeys the Curie−Weiss law, $\chi_M = C/(T-\theta)$ in the whole temperature range with the Weiss constant, θ, of −19.381 K and the Curie constant, C_{M_2} of 4.39 cm^3 K mol^{-1}. At 300 K, the $\chi_M T$ value is 4.11 cm^3 K mol^{-1} (5.73 μB), which is slightly below the expected value of 4.38 cm^3 K mol^{-1} (5.92 μB) for magnetically isolated high-spin Mn(II) ($S_{Mn} = 5/2$, $g = 2.0$). This value decreases smoothly to 0.444 cm^3 K mol^{-1} at 2 K. The rapid decreases of $\chi_M T$ below 70 K and the negative θ value are attributed to antiferromagnetic interactions between Mn(II) centers in polymer **3**.

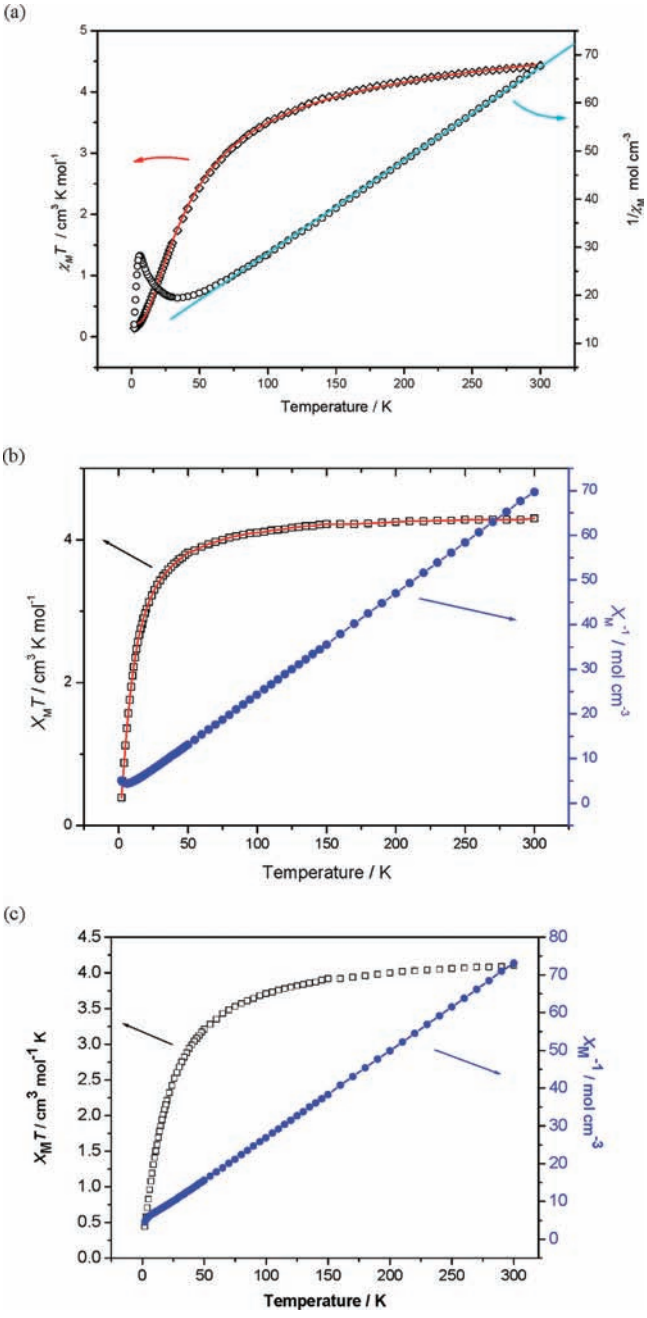

Figure 6. Plots of experimental $\chi_M T$ vs T and $1/\chi_M$ vs T of (a) **1**, (b) **2**, and (c) **3**.

As is mentioned in the crystallographic part, the 2D structure of **3** can be viewed as chains linked by organic ligands. Thus, we tried to theoretically fit the experimental data by the equation as in the case of polymer **2**. Unfortunately, we could not get a satisfactory result. Obviously, the magnetic pathways between neighbor Mn(II) ions of **3** are complicated, which could not be simply dealt with as the case in **2**. However, compared

(23) (a) Yao, Y. L.; Che, Y. X.; Zheng, J. M. *Cryst. Growth Des.* **2008**, *8*, 2299. (b) Liu, B. L.; Xiao, H.-P.; Nfor, E. N.; Song, Y.; You, X. Z. *Inorg. Chem. Commun.* **2009**, *12*, 8.
(24) Fisher, M. E. *Am. J. Phys.* **1963**, *32*, 343.
(25) Wagner, G. R.; Friedberg, S. A. *Phys. Lett.* **1964**, *9*, 11.
(26) McElearney, J. N.; Merchant, S.; Carlin, R. L. *Inorg. Chem.* **1973**, *12*, 906.

with the Weiss constant of **2** and **3** (θ: −10.438 and −19.381 K, respectively), it is obvious that the antiferromagnetic coupling in **3** is stronger than that in **2**, which mainly results from the difference between their structures.

Because Cd(II) ion has no unpaired electrons, complex **4** is expected to be diamagnetic.

Conclusion

In summary, a series of novel metal−organic complexes with architectural diversity has been successfully synthesized under hydro(solvo)thermal conditions by fine control over solvent and pH values. The organic ligand H_3EIDC displays various coordination modes, which can generate interesting structures with metal ions ranging from molecular square and two- to three-dimensional pillared layer structures. Compounds **1**−**3** all show antiferromagnetic interactions between the neighbor metal centers.

Acknowledgment. We gratefully acknowledge the financial support by the National Natural Science Foundation of China (20501017) and by the Key Project of Chinese Ministry of Education (207067). We acknowledge the project sponsored by the Scientific Research Foundation for the Returned Overseas Chinese Scholars of Chinese Ministry of Education and the Natural Science Foundation of Henan Education Department (2007150040; 2009A150028) and Associate Professor Qingling Meng for helpful advice.

Supporting Information Available: Crystallographic data in CIF and pdf formats. This material is available free of charge via the Internet at http://pubs.acs.org.